

Influence of transverse interdot coupling on transport properties of an Aharonov-Bohm structure composed by two dots and two reservoirs

Z. T. Jiang,^{1,*} J. Q. You,^{1,2} S. B. Bian,¹ and H. Z. Zheng¹

¹National Laboratory for Superlattices and Microstructures, Institute of Semiconductors, Chinese Academy of Sciences, P.O. Box 912, Beijing 100083, People's Republic of China

²Frontier Research System, The Institute of Physical and Chemical Research (RIKEN), Wako-shi 351-0198, Japan

(Received 22 April 2002; revised manuscript received 24 July 2002; published 7 November 2002)

We derive the modified rate equations for an Aharonov-Bohm (AB) ring with two transversely coupled quantum dots (QD's) embedded in two arms in the presence of a magnetic field. We find that the interdot coupling between the two QD's can cause a temporal oscillation in electron occupation at the initial stage of the quantum dynamics, while the source-drain current decays monotonically to a stationary value. On the other hand, the interdot coupling equivalently divides the AB ring into two coupled subrings. That also destroys the normal AB oscillations with a period of 2π , and generates new and complex periodic oscillations with their periods varying in a linear manner as the ratio between two magnetic fluxes (each penetrates one AB subring) increases. Furthermore, the interference between two subrings is also evident from the observation of the perturbed fundamental AB oscillation.

DOI: 10.1103/PhysRevB.66.205306

PACS number(s): 73.63.-b, 03.65.Yz, 03.65.Vf

I. INTRODUCTION

Recent advances in nanotechnologies have made it possible to fabricate quantum dot (QD) structures with geometrical dimensions smaller than the elastic mean free paths. Therefore, electron transport in such small structures is ballistic and its phase coherence can be sustained. Many studies on the coherence in a coupled QD system have been performed both experimentally¹⁻³ and theoretically.⁴⁻⁹ Yacoby *et al.*¹⁰ and Schuster *et al.*¹¹ reported the experimental observations of the transmission phase through a QD embedded in one arm of the Aharonov-Bohm (AB) ring. In this setup, the dephasing induced by a "which-path" detector has also been investigated by Buks *et al.*¹² Their study shows that the visibility of the oscillatory signal is affected by the sensitivity of the detector, which verifies the complementary principle for fermions. Very recently, Holleitner *et al.*¹³ measured the AB oscillations of the mesoscopic ring with a QD inserted in each arm, and found that they displayed the magnetic-field dependence of the coherently coupled states. Theoretically, this has been discussed by König and Gefen.¹⁴ Also, Loss and Sukhorukov¹⁵ theoretically studied the phase-coherent current in vertically coupled QD's. However, these studies have not yet explicitly shown the quantum transient dynamics of the coupled QD system.

Using modified rate equations, Gurvitz and co-worker^{16,17} systematically investigated the transport properties and the dephasing in horizontally coupled multiple QD systems. Motivated by this work, we study here a transversely coupled QD structure embedded in an AB ring, which is then sandwiched between source and drain reservoirs by Gurvitz's methods. We derive the modified rate equations for this system in the presence of a magnetic field. First, we show the temporary evolutions of the electron-occupation probabilities in all states, and find that the tunneling of electrons back and forth between dots 1 and 2 is going to cause a temporal oscillation at the initial stage of the quantum dynamics in the

case of zero magnetic field. Then, we study the quantum dynamics of the coupled QD system in the presence of a magnetic field, and reveal that the AB oscillations of the current, flowing through the two-coupled-QD structure, can still be observed even in the stationary case, where the electron-occupation probabilities in all states are constant. Also, it is shown that by forming two coupled subrings the interdot coupling destroys the 2π -period oscillation of the stationary current and generates a new periodic oscillation. Its period, independent of the strength of the interdot coupling and the tunneling rates between QD's and reservoirs, increases in a linear manner as the ratio between two magnetic fluxes (each penetrates one AB subring divided by the interdot coupling) increases. On the other hand, the interference between two subrings is also evident from the observation of the perturbed fundamental AB oscillation.

II. THEORY

The coupled-QD system that we study here is schematically illustrated in Fig. 1. A mesoscopic ring is connected by two reservoirs (source and drain), with two QD's (dot 1 and

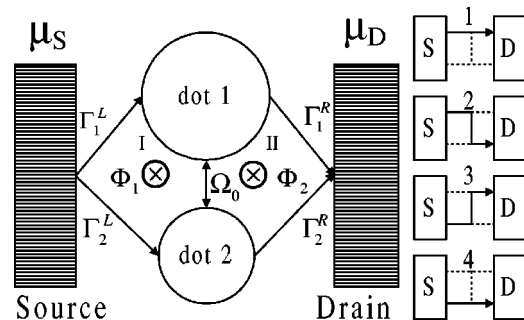


FIG. 1. Schematic illustration of the coupled-quantum-dot structure sandwiched between two reservoirs, where Ω_0 denotes the interdot coupling. The right part shows the four classical channels for electrons to flow from the source to the drain.

dot 2) inserted, one dot in each arm. The chemical potentials of the source and the drain are denoted by μ_S and μ_D , respectively. Γ_1^L (Γ_2^L) and Γ_1^R (Γ_2^R) represent the rates of electron transitions from the source to dot 1 (dot 2) and from dot 1 (dot 2) to the drain. The interdot coupling Ω_0 between dots 1 and 2 divides the mesoscopic ring into two subrings (I and II). Through each subring there exist the magnetic fluxes Φ_1 and Φ_2 threaded, respectively. In the presence of a magnetic field, the Hamiltonian of the coupled QD system with source and drain reservoirs included can be written as^{16,18}

$$H = \sum_{i=1,2,l,r} E_i a_i^\dagger a_i + \Omega_0 (e^{i\phi_{12}} a_2^\dagger a_1 + \text{H.c.}) + \sum_{j=l,r} (T_{j1} e^{i\phi_{j1}} a_1^\dagger a_j + T_{j2} e^{i\phi_{j2}} a_2^\dagger a_j + \text{H.c.}). \quad (1)$$

Here a_i^\dagger (a_i) is the electron creation (annihilation) operator for the basis state $|i\rangle$, and l (r) labels source (drain) reservoir. T_{j1} (T_{j2}) represents the coupling between dot 1 (dot 2) and the reservoir j ($j=l, r$), ϕ_{j1} (ϕ_{j2}) is the phase of the path from reservoir j to dot 1 (dot 2), and ϕ_{12} is the total phase of the path from dot 1 to dot 2. It is evident that the total magnetic flux Φ through the mesoscopic ring is equal to $\Phi_1 + \Phi_2$, and the corresponding reduced flux is defined by $\phi = \phi_1 + \phi_2 = 2\pi\Phi/\Phi_0$, with $\phi_1 = \phi_{l1} + \phi_{l2} - \phi_{r2}$, and $\phi_2 = -\phi_{r1} - \phi_{l2} + \phi_{r2}$.

As shown in the right part of Fig. 1, there are four classical channels 1, 2, 3, and 4 for the electron to transport from the source to the drain. The phases accumulated in these channels are denoted by $P_1 = \phi_{l1} - \phi_{r1}$, $P_2 = \phi_{l1} + \phi_{l2} - \phi_{r2}$, $P_3 = \phi_{l2} - \phi_{l2} - \phi_{r1}$, and $P_4 = \phi_{l2} - \phi_{r2}$, respectively. The possible phase differences between two of them are

$$\phi_A = P_1 - P_2 = P_3 - P_4 = -\phi_{r1} - \phi_{l2} + \phi_{r2}, \quad (2a)$$

$$\phi_B = P_1 - P_3 = P_2 - P_4 = \phi_{l1} + \phi_{l2} - \phi_{l2}, \quad (2b)$$

$$\phi_C = P_1 - P_4 = \phi_{l1} - \phi_{r1} - \phi_{l2} + \phi_{r2}, \quad (2c)$$

$$\phi_D = P_2 - P_3 = \phi_{l1} - \phi_{l2} + 2\phi_{l2} + \phi_{r1} - \phi_{r2}. \quad (2d)$$

Thus the current through the coupled-QD system should include the sum of the cosine functions of these phase differences since the electrons, traveling through the four channels, are going to interfere with each other.¹⁹

For simplicity, our discussion is restricted to the zero-temperature case, and the system initially remains in a vacuum state $|0\rangle$, where the states of the source and the drain are filled up to their Fermi levels, respectively. The wave function of the entire system can be expressed in the occupation number representation as^{16,17}

$$|\Psi(t)\rangle = \left[b_0(t) + \sum_{lr} b_{lr}(t) a_r^\dagger a_l + \sum_{l<l', r<r'} b_{ll'rr'}(t) a_r^\dagger a_r^\dagger a_{l'} a_l + \sum_l b_{l1}(t) a_1^\dagger a_l + \sum_{l<l', r} b_{ll'1r}(t) a_1^\dagger a_1^\dagger a_l a_{l'} + \sum_l b_{l2}(t) a_2^\dagger a_l + \sum_{l<l', r} b_{ll'2r}(t) a_2^\dagger a_2^\dagger a_r a_{l'} + \sum_{l<l'} b_{ll'12}(t) a_1^\dagger a_2^\dagger a_l a_{l'} + \dots \right] |0\rangle, \quad (3)$$

where $b(t)$ are the time-dependent amplitudes of finding the electron in the states defined by the corresponding creation and annihilation operators. The quantum evolution of the whole system is described by the Schrödinger equation $i|\dot{\Psi}\rangle = H|\Psi\rangle$. In the four-dimensional Fock space, consisting of states $|a\rangle$, $|b\rangle$, $|c\rangle$, and $|d\rangle$ (in these states or levels, E_1 and E_2 are both empty, only E_1 is occupied, only E_2 is occupied, and both E_1 and E_2 are occupied, respectively), the elements of the density matrix $\sigma(t) = |\Psi(t)\rangle\langle\Psi(t)|$ can be written as

$$\dot{\sigma}_{aa}^n = -(\Gamma_1^L + \Gamma_2^L) \sigma_{aa}^n + \Gamma_1^R \sigma_{bb}^{n-1} + \Gamma_2^R \sigma_{cc}^{n-1} + e^{i(\phi_{r1} - \phi_{r2})} \Gamma_{12}^R \sigma_{cb}^{n-1} + e^{-i(\phi_{r1} - \phi_{r2})} \Gamma_{12}^R \sigma_{bc}^{n-1}, \quad (4a)$$

$$\begin{aligned} \dot{\sigma}_{bb}^n &= -(\Gamma_2^L + \Gamma_1^R) \sigma_{bb}^n + i\Omega_0 (e^{i\phi_{12}} \sigma_{bc}^n - e^{-i\phi_{12}} \sigma_{cb}^n) \\ &\quad - [e^{-i(\phi_{l1} - \phi_{l2})} \Gamma_{12}^L + e^{-i(\phi_{r1} - \phi_{r2})} \Gamma_{12}^R] \sigma_{bc}^n / 2 \\ &\quad - [e^{i(\phi_{l1} - \phi_{l2})} \Gamma_{12}^L + e^{i(\phi_{r1} - \phi_{r2})} \Gamma_{12}^R] \sigma_{cb}^n / 2 \\ &\quad + \Gamma_1^L \sigma_{aa}^n + \Gamma_2^R \sigma_{dd}^{n-1}, \end{aligned} \quad (4b)$$

$$\begin{aligned} \dot{\sigma}_{cc}^n &= -(\Gamma_1^L + \Gamma_2^R) \sigma_{cc}^n + i\Omega_0 (e^{-i\phi_{12}} \sigma_{cb}^n - e^{i\phi_{12}} \sigma_{bc}^n) \\ &\quad - [e^{-i(\phi_{l1} - \phi_{l2})} \Gamma_{12}^L + e^{-i(\phi_{r1} - \phi_{r2})} \Gamma_{12}^R] \sigma_{bc}^n / 2 \\ &\quad - [e^{i(\phi_{l1} - \phi_{l2})} \Gamma_{12}^L + e^{i(\phi_{r1} - \phi_{r2})} \Gamma_{12}^R] \sigma_{cb}^n / 2 \\ &\quad + \Gamma_2^L \sigma_{aa}^n + \Gamma_1^R \sigma_{dd}^{n-1}, \end{aligned} \quad (4c)$$

$$\begin{aligned} \dot{\sigma}_{dd}^n &= -(\Gamma_1^R + \Gamma_2^R) \sigma_{dd}^n + \Gamma_1^L \sigma_{cc}^n + \Gamma_2^L \sigma_{bb}^n + e^{i(\phi_{l1} - \phi_{l2})} \Gamma_{12}^L \sigma_{cb}^n \\ &\quad + e^{-i(\phi_{l1} - \phi_{l2})} \Gamma_{12}^L \sigma_{bc}^n, \end{aligned} \quad (4d)$$

$$\begin{aligned} \dot{\sigma}_{bc}^n &= i\varepsilon \sigma_{bc}^n + ie^{-i\phi_{12}} \Omega_0 (\sigma_{bb}^n - \sigma_{cc}^n) - (\Gamma_1^L + \Gamma_2^R + \Gamma_2^L \\ &\quad + \Gamma_1^R) \sigma_{bc}^n / 2 - [e^{i(\phi_{l1} - \phi_{l2})} \Gamma_{12}^L + e^{i(\phi_{r1} - \phi_{r2})} \Gamma_{12}^R] \\ &\quad \times (\sigma_{bb}^n + \sigma_{cc}^n) / 2. \end{aligned} \quad (4e)$$

Here the index n denotes the electron number in the drain and $\varepsilon = E_2 - E_1$ is the energy detuning between dots 1 and 2. $\Gamma_1^L = 2\pi T_{l1}^2 \rho_L$ ($\Gamma_2^L = 2\pi T_{l2}^2 \rho_L$) and $\Gamma_1^R = 2\pi T_{r1}^2 \rho_R$

($\Gamma_2^R = 2\pi T_{r2}^2 \rho_R$) are the rates of the electron tunneling into dot 1 (dot 2) from the source and out of dot 1 (dot 2) into the drain. The coherent terms are given by $\Gamma_{12}^L = 2\pi T_{l1} T_{l2} \rho_L = \sqrt{\Gamma_1^L \Gamma_2^L}$ and $\Gamma_{12}^R = 2\pi T_{r1} T_{r2} \rho_R = \sqrt{\Gamma_1^R \Gamma_2^R}$. By summing up over n in Eqs. (4) we obtain the time-dependent reduced density matrices of the whole system,

$$\dot{\sigma}_{aa} = -(\Gamma_1^L + \Gamma_2^L)\sigma_{aa} + \Gamma_1^R \sigma_{bb} + \Gamma_2^R \sigma_{cc} + e^{i(\phi_{r1} - \phi_{r2})} \Gamma_{12}^R \sigma_{bc} + e^{-i(\phi_{r1} - \phi_{r2})} \Gamma_{12}^R \sigma_{cb}, \quad (5a)$$

$$\dot{\sigma}_{bb} = -(\Gamma_2^L + \Gamma_1^R)\sigma_{bb} + i\Omega_0(e^{i\phi_{12}}\sigma_{bc} - e^{-i\phi_{12}}\sigma_{cb}) + \Gamma_1^L \sigma_{aa} + \Gamma_2^R \sigma_{dd} - [e^{-i(\phi_{l1} - \phi_{l2})} \Gamma_{12}^L + e^{-i(\phi_{r1} - \phi_{r2})} \Gamma_{12}^R] \sigma_{bc}/2 - [e^{-i(\phi_{l1} - \phi_{l2})} \Gamma_{12}^L + e^{i(\phi_{r1} - \phi_{r2})} \Gamma_{12}^R] \sigma_{cb}/2, \quad (5b)$$

$$\dot{\sigma}_{cc} = -(\Gamma_1^L + \Gamma_2^R)\sigma_{cc} + i\Omega_0(e^{-i\phi_{12}}\sigma_{cb} - e^{i\phi_{12}}\sigma_{bc}) + \Gamma_2^L \sigma_{aa} + \Gamma_1^R \sigma_{dd} - [e^{-i(\phi_{l1} - \phi_{l2})} \Gamma_{12}^L + e^{-i(\phi_{r1} - \phi_{r2})} \Gamma_{12}^R] \sigma_{bc}/2 - [e^{i(\phi_{l1} - \phi_{l2})} \Gamma_{12}^L + e^{i(\phi_{r1} - \phi_{r2})} \Gamma_{12}^R] \sigma_{cb}/2, \quad (5c)$$

$$\dot{\sigma}_{dd} = -(\Gamma_1^R + \Gamma_2^R)\sigma_{dd} + \Gamma_2^L \sigma_{bb} + \Gamma_1^L \sigma_{cc} + e^{i(\phi_{l1} - \phi_{l2})} \Gamma_{12}^L \sigma_{cb} + e^{-i(\phi_{l1} - \phi_{l2})} \Gamma_{12}^L \sigma_{bc}, \quad (5d)$$

$$\dot{\sigma}_{bc} = i\varepsilon \sigma_{bc} + i\Omega_0 e^{-i\phi_{12}}(\sigma_{bb} - \sigma_{cc}) - (\Gamma_1^L + \Gamma_2^R + \Gamma_2^L + \Gamma_1^R) \sigma_{bc}/2 - [e^{i(\phi_{l1} - \phi_{l2})} \Gamma_{12}^L + e^{i(\phi_{r1} - \phi_{r2})} \Gamma_{12}^R] \sigma_{cb}/2 \times (\sigma_{bb} + \sigma_{cc})/2. \quad (5e)$$

The diagonal matrix σ_{ii} ($i=a, b, c$, and d) represents the probability of finding the electron in the corresponding state $|i\rangle$ and obeys the probability conservation $\sum_i \sigma_{ii} = 1$. Because of the last term in Eq. 5(e), the nondiagonal density-matrix element σ_{bc} shows different behaviors of damping, as compared with the horizontally coupled QD system.^{16,20} The total current, flowing from the source to the drain, can be derived as

$$I(t) = I_C + I_D = e \sum_n n (\dot{\sigma}_{aa}^n + \dot{\sigma}_{bb}^n + \dot{\sigma}_{cc}^n + \dot{\sigma}_{dd}^n), \quad (6)$$

where the magnetocurrent is given by

$$I_C = e \Gamma_{12}^R [e^{i(\phi_{r1} - \phi_{r2})} \sigma_{cb} + \text{H.c.}], \quad (7)$$

and the direct current is

$$I_D = e [\Gamma_1^R \sigma_{bb} + \Gamma_2^R \sigma_{cc} + (\Gamma_1^R + \Gamma_2^R) \sigma_{dd}], \quad (8)$$

which is not apparently related to the magnetic field. Furthermore, the magnetocurrent can be written as $2e \eta \Gamma_{12}^R \cos(\phi_{r1} - \phi_{r2} + \Delta)$ if we assume the coherent term to be $\sigma_{bc} = \eta e^{i\Delta}$.

III. NUMERICAL CALCULATIONS AND DISCUSSION

In what follows, we numerically solve Eqs. 5(a)–5(e) to explore the quantum dynamical behavior of the coupled QD system. In our calculations, the energy detuning ε between

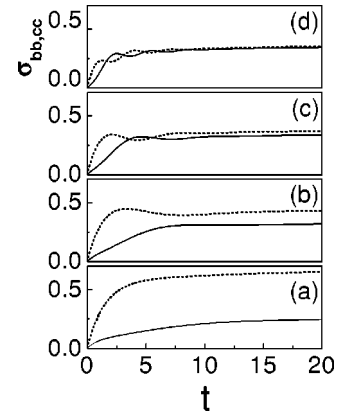


FIG. 2. Electron-occupation probabilities σ_{bb} (dotted) and σ_{cc} (solid) as a function of time t (in units of $1/\Omega_0$) for different interdot couplings (a) $\Omega_0=0$, (b) $\Omega_0=0.25$, (c) $\Omega_0=0.5$, and (d) $\Omega_0=1$. The parameters used for calculations are $\Gamma_1^L=0.4$ and $\Gamma_1^R=\Gamma_2^R=0.1$.

the two dots is kept 0. The two subrings (I and II) of the mesoscopic AB ring are threaded by magnetic fluxes Φ_1 and Φ_2 , respectively. The phases associated with these two subrings are written as $\phi_1 = \Delta\phi_l + \phi_{12}$ and $\phi_2 = \Delta\phi_r - \phi_{12}$, with $\Delta\phi_l = \phi_{l1} - \phi_{l2}$ and $\Delta\phi_r = \phi_{r2} - \phi_{r1}$. Here we choose $\phi_1/\phi_2 = \Delta\phi_1/\Delta\phi_2$ with $\phi_{12}=0$ and the tunneling rates $\Gamma_1^L=0.4$ and $\Gamma_1^R=\Gamma_2^R=0.1$.

First, we investigate the quantum dynamics of the coupled QD system in the case of zero magnetic field, as shown in Fig. 2. Time dependences of the electron-occupation probabilities σ_{bb} and σ_{cc} in states $|b\rangle$ and $|c\rangle$ are shown with dotted and solid curves. When the interdot coupling $\Omega_0=0$, the probability σ_{bb} is larger than σ_{cc} at $t \neq 0$ because a stronger coupling Γ_1^L will guide electrons to enter dot 1 faster [see Fig. 2(a)]. Figures 2(b–d) display the probability evolutions for the different interdot couplings $\Omega_0=0.25$, 0.5 , and 1 , respectively. It is shown that these curves exhibit temporal oscillations at small t , which indicates that the electron tunnels back and forth between dots 1 and 2. By a close look, one can find that the oscillation period of the curves in Fig. 2(c) is twice that in Fig. 2(d). This is in accordance with the relations²¹ $|a(t)|^2 = \cos^2(\Omega_0 t)$ and $|b(t)|^2 = \sin^2(\Omega_0 t)$, which reveals that the oscillation period will be shortened by increasing the interdot coupling. Also, one can see that probabilities σ_{bb} and σ_{cc} become constant after sufficiently long time, indicating that the coupled QD system has evolved into a stationary state. Numerical results also show that the probability σ_{aa} decreases and σ_{dd} increases at the initial stage and they become constant in the stationary case, which are not plotted in the present paper.

In Fig. 3, we plot the current flowing from the source to the drain as a function of t in the absence of a magnetic field. For the sake of comparison, the currents through the single-dot structure [see the inset to Fig. 3(a)] and horizontal double-dot structure [see the inset to Fig. 3(b)] are also shown in Figs. 3(a) and 3(b), respectively, where the tunneling rates between QD's and reservoirs are chosen to be 0.1 and the interdot coupling is 1 . Both of the currents, through these two kinds of structures, become constant at large

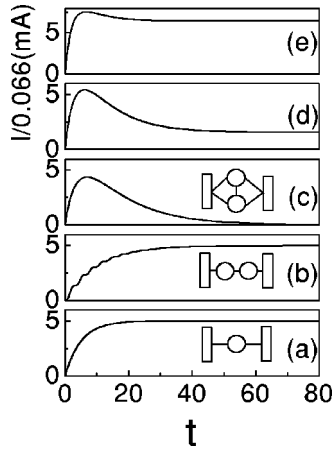


FIG. 3. Evolutions of the currents through the single-dot structure (a), horizontal double-dot structure (b), and transverse double-dot structure for different tunneling rates (c) $\Gamma_1^L=0.1$, (d) 0.2, and (e) 0.4. The interdot coupling is selected to be 1 and $\Gamma_1^R=\Gamma_2^L=\Gamma_2^R=0.1$. The time t is in units of $1/\Omega_0$.

t when the states of the systems become stationary. Also, we can see that the current through the horizontal double-dot structure exhibits transient oscillations at small t , which stems from the coupling between the double QD's. Very different from the above two cases, the current through the transversely coupled double-dot structure [see the inset to Fig. 3(c)] shows only one single peak when the tunneling rate $\Gamma_1^L=0.1$ [see Fig. 3(c)]. The current I decays eventually to zero at large time t . This is because that the π -phase results in $I_C=-2\eta\Gamma_{12}^R$, equal the current $-I_D$. When the tunneling rate Γ_1^L takes a value of 0.2, the current at large time ($t>60$) becomes non-zero constant, equal to $1.56 (\times 0.066 \text{ mA})$, which will, hereafter, be called the stationary current. On increasing the tunneling rate Γ_1^L further, the stationary current also increases as shown by the curve in Fig. 3(e). This can be understood from a physical point of view. When all the tunneling rates take the same values, e.g., 0.1, the electrons mainly arrive at the drain through channels 1 and 4 with the amplitude $A_1=A_4$ and the phase difference $\Delta=\pi$, which yields the zero current flowing from the source to the drain. While the tunneling rate Γ_1^L takes 0.4, the other two channels, 2 and 3, become open, and the amplitude A_1 becomes larger than A_4 with the corresponding phase becoming small. This leads to the increase in the stationary current, analogous to the electron double-slit experiment.

We then study the stationary current flowing from the source to the drain in the presence of a magnetic field. Figure 4 displays the currents I for different interdot couplings at $t=80$ under the conditions $\Phi_1=2\Phi_2$, $\Gamma_1^L=0.1$, (solid curves) and $\Gamma_1^L=0.4$ (dotted curves). It is clear that the currents shown by the dotted curves are larger than those by the solid ones at the same reduced flux ϕ and interdot coupling Ω_0 , verifying that the stationary current increases as the tunneling rate becomes large. In the absence of the interdot coupling ($\Omega_0=0$), the stationary currents I exhibit periodic oscillations with a period of 2π . This is just the main feature of the common AB effect. However, the first current peak

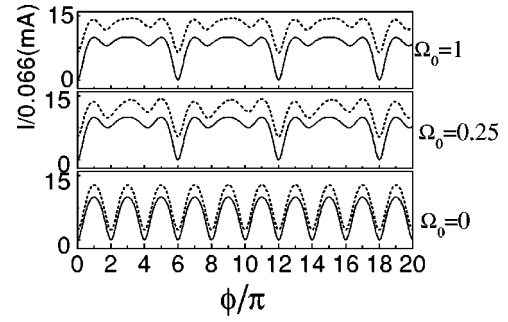


FIG. 4. Variations of the stationary currents I as a function of the reduced flux ϕ for different tunneling rates $\Gamma_1^L=0.1$ (solid) and 0.4 (dotted) with $\Phi_1=2\Phi_2$ and $\Gamma_1^R=\Gamma_2^L=\Gamma_2^R=0.1$.

appears at the phase of π . This fact verifies again that there is an accumulating phase π around the mesoscopic ring even in the absence of a magnetic field. In sharp contrast, the features of the mesoscopic transport change substantially as the interdot coupling turns on in our AB ring. As clearly shown in Fig. 4, the fundamental 2π -period oscillation becomes weakened, and its periodicity (2π) is also disturbed a little bit. At the same time, a new and complex oscillation appears with a period of 6π . Obviously, the latter stems from the AB effect of the AB subring threaded by flux Φ_2 , since $\Phi_2=(\Phi_1+\Phi_2)/3$. From Fig. 4, one is also aware that such perturbed AB oscillations keep their main characteristics unchanged, and are irrespective of the interdot coupling strength and the tunneling rates between the reservoirs and QD's.

Therefore, we further investigate the periodicity of the stationary currents for different flux ratios Φ_1/Φ_2 with $\Omega_0=1$ in Fig. 5. When $\Phi_1=\Phi_2$, the stationary current shows periodic oscillations with a period of 4π . In this case the AB oscillations associated with the two AB subrings (threaded by $\Phi_1=\Phi_2=\Phi/2$, respectively) are commensurable to the fundamental AB oscillation, because the former has a periodicity of 4π and the latter has a periodicity of 2π . As a result, it is not easy to discern the 4π -period oscillation with the 2π -period oscillation. One also can see clearly that it evolves into the oscillation with the period of 6π , 8π , and 10π in response to different flux ratios, $\Phi_1/\Phi_2=2, 3$, and 4. It should be pointed out that whenever $\Phi=\Phi_1+\Phi_2$ becomes

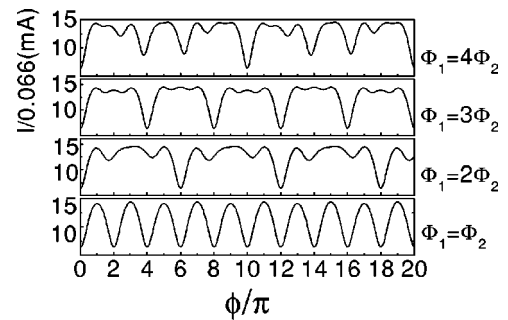


FIG. 5. Variations of the stationary currents as a function of the reduced flux ϕ for different magnetic flux ratios. The interdot coupling is selected to be 1 and the tunneling rates are $\Gamma_1^L=0.4$ and $\Gamma_1^R=\Gamma_2^L=\Gamma_2^R=0.1$.

even times of Φ_2 (e.g., $\Phi_1/\Phi_2=1,3,5,\dots$), the mentioned commensurability makes it difficult to distinguish, for example, 8π -period oscillation from 4π -period one. On the other hand, due to the interference between the channels 2 and 3 (see the right part in Fig. 1) the fundamental 2π -period oscillation is also disturbed substantially as seen in the case of $\Phi_1=4\Phi_2$. If we assume $\Phi_1/\Phi_2=n$, the total phases associated with the two subrings of the mesoscopic ring can be expressed as follows:

$$\phi_1 = \frac{n}{n+1} \phi, \quad \phi_2 = \frac{1}{n} \phi,$$

where $\phi=2\pi\Phi/\Phi_0$. Thus, the phases associated with the transports in the legs of the mesoscopic ring are given by

$$\phi_{l1} = -\phi_{l2} = \frac{n}{2(n+1)} \phi$$

and

$$\phi_{r1} = -\phi_{r2} = -\frac{1}{2(n+1)} \phi.$$

Correspondingly, the possible phase differences are expressed as ϕ , $1/(n+1)\phi$, $n/(n+1)\phi$, and $(n-1)/(n+1)\phi$. Therefore, the oscillating periods equal 2π , $2(n+1)\pi$, $2(n+1)\pi/n$, and $2(n+1)\pi/(n-1)$, respectively, indicating that the period should be $2(n+1)\pi$. This verifies that the oscillation period increases in a linear manner with increasing the magnetic flux ratio n .

IV. SUMMARY

In summary, we have derived the modified rate equations for a mesoscopic ring with two transversely coupled QD's inserted in the two arms when a perpendicular magnetic field is applied. We show the temporary evolutions of the electron-occupation probabilities in all states and find that the tunneling of electrons back and forth between dots 1 and 2 is going to cause a temporal oscillation at the initial stage of the quantum dynamics. On the other hand, the currents flowing from the source to the drain become constant after sufficiently long time, implying that the coupled QD system eventually evolves into a stationary state. Furthermore, we investigate the transport properties of the stationary system in the presence of a magnetic field. We find that by forming two coupled subrings the interdot coupling destroys the 2π -period oscillation as conventionally observed in the typical AB effect and generates new oscillations with their periods increasing linearly when the magnetic flux ratio increases. The interference between two subrings is also evident from the observation of the perturbed fundamental AB oscillation.

ACKNOWLEDGMENTS

This work was supported by the National Natural Science Foundation of China under Grants Nos. 10174075 and G001CB3095-1. J.Q.Y. is also supported by the Frontier Research System at RIKEN, Japan.

*Email address: ztjiang@red.semi.ac.cn;
jiangzhaotan@hotmail.com

- ¹F. R. Waugh, M. J. Berry, D. J. Mar, R. M. Westervelt, K. L. Campman, and A. C. Gossard, Phys. Rev. Lett. **75**, 705 (1995).
- ²N. C. van der Vaart, S. F. Godijn, Y. V. Nazarov, C. J. P. M. Harmans, J. E. Mooij, L. W. Molenkamp, and C. T. Foxon, Phys. Rev. Lett. **74**, 4702 (1995); R. H. Blick, R. J. Haug, J. Weis, D. Pfannkuche, K. v. Klitzing, and K. Eberl, Phys. Rev. B **53**, 7899 (1996).
- ³T. H. Oosterkamp, T. Fujisawa, W. G. vander Wiel, K. Ishibashi, R. V. Hijman, S. Tarucha, and L. P. Kouwenhoven, Nature (London) **395**, 873 (1998).
- ⁴C. A. Stafford and N. S. Wingreen, Phys. Rev. Lett. **76**, 1916 (1996).
- ⁵G. Klimeck, G. Chen, and S. Datta, Phys. Rev. B **50**, 2316 (1994); G. Chen, G. Klimeck, S. Datta, G. Chen, and W. A. Goodard *ibid.* **50**, 8035 (1994).
- ⁶F. Ramirez, E. Cota, and S. E. Ulloa, Phys. Rev. B **59**, 5717 (1999); C. Niu, L.-J. Liu, and T.-H. Lin, *ibid.* **51**, 5130 (1995).
- ⁷J. Q. You and H. Z. Zheng, Phys. Rev. B **60**, 13 314 (1999).
- ⁸R. H. Blick, D. Pfannkuche, R. J. Haug, K. v. Klitzing, and K. Eberl, Phys. Rev. Lett. **80**, 4032 (1998).
- ⁹I. L. Aleiner, N. S. Wingreen, and Y. Meir, Phys. Rev. Lett. **79**, 3740 (1997).
- ¹⁰A. Yacoby, M. Heiblum, D. Mahalu, and H. Shtrikman, Phys.

- Rev. Lett. **74**, 4047 (1995); A. Yacoby, R. Schuster, and M. Heiblum, Phys. Rev. B **53**, 9583 (1996).
- ¹¹R. Schuster, E. Buks, M. Heiblum, D. Mahalu, V. Umansky, and H. Shtrikman, Nature (London) **385**, 417 (1997).
- ¹²E. Buks, R. Schuster, M. Heiblum, D. Mahalu, and V. Umansky, Nature (London) **391**, 871 (1998).
- ¹³A. W. Holleitner, C. R. Decker, H. Qin, K. Eberl, and R. H. Blick, Phys. Rev. Lett. **87**, 256802 (2001).
- ¹⁴J. König and Y. Gefen, Phys. Rev. B **65**, 045316 (2002).
- ¹⁵D. Loss and E. V. Sukhorukov, Phys. Rev. Lett. **84**, 1035 (2000).
- ¹⁶S. A. Gurvitz, Phys. Rev. B **57**, 6602 (1998); Phys. Rev. Lett. **85**, 812 (2000).
- ¹⁷S. A. Gurvitz and Ya. S. Prager, Phys. Rev. B **53**, 15 932 (1996).
- ¹⁸G. Hackenbroich and H. A. Weidenmüller, Phys. Rev. B **53**, 16 379 (1996); Phys. Rev. Lett. **76**, 110 (1996).
- ¹⁹It is assumed that the wave functions of the electrons through channels 1, 2, 3, and 4 to the drain are $A_1 e^{iP_1}$, $A_2 e^{iP_2}$, $A_3 e^{iP_3}$, and $A_4 e^{iP_4}$, respectively. The total wave function in the drain can be written as $|\Psi_D\rangle = \sum_{m=1}^4 A_m e^{iP_m}$. Therefore, the probability of the electron is $\rho = \langle \Psi_D | \Psi_D \rangle = \sum_{m=1}^4 |A_m|^2 + \sum_{m=1}^4 \sum_{n(\neq m)=1}^4 [2A_m A_n^* \cos(P_m - P_n)]$.
- ²⁰Z. T. Jiang, J. Peng, J. Q. You, and H. Z. Zheng, Phys. Rev. B **65**, 153308 (2002).
- ²¹N. Tsukada, A. D. Wieck, and K. Ploog, Appl. Phys. Lett. **56**, 2527 (1990).